Short Article

Cell Stem Cell

Inhibition of Aberrant DNA Re-methylation Improves Post-implantation Development of Somatic Cell Nuclear Transfer Embryos

Graphical Abstract

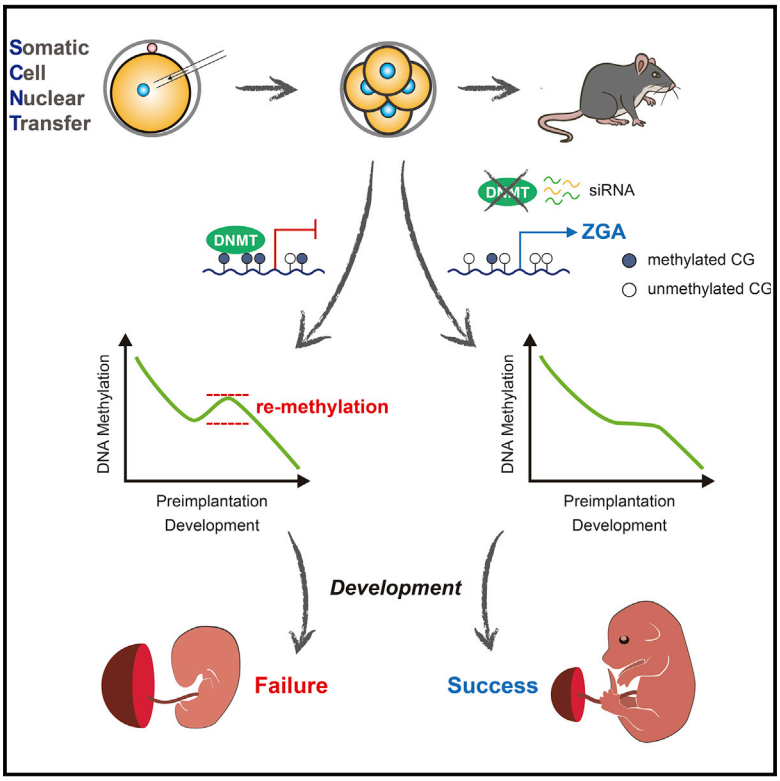

Authors

Rui Gao, Chenfei Wang, Yawei Gao, ..., Wenqiang Liu, Yong Zhang, Shaorong Gao

Correspondence

liuwenqiang@tongji.edu.cn (W.L.), yzhang@tongji.edu.cn (Y.Z.), gaoshaorong@tongji.edu.cn (S.G.)

In Brief

Gao et al. show that aberrant DNA re-methylation is a critical epigenetic barrier to SCNT embryo development. Inactivation of Dnmts can rescue re-methylation defects and improve post-implantation development of SCNT embryos and overall cloning efficiency, which is further enhanced by simultaneous removal of additional epigenetic barriers.

Highlights

- Genome-wide maps reveal atypical DNA re-methylation in pre-implantation SCNT embryos
- DNA re-methylation disrupts normal zygotic genome activation in SCNT embryos
- Dnmt knockdown alleviates re-methylation and improves SCNT embryo development
- Combined Dnmt inhibition and Kdm overexpression improves cloning efficiency

Gao et al., 2018, Cell Stem Cell *23*, 1–10
September 6, 2018
https://doi.org/10.1016/j.stem.2018.07.017

CellPress

Please cite this article in press as: Gao et al., Inhibition of Aberrant DNA Re-methylation Improves Post-implantation Development of Somatic Cell Nuclear Transfer Embryos, Cell Stem Cell (2018), https://doi.org/10.1016/j.stem.2018.07.017

Cell Stem Cell
Short Article

Inhibition of Aberrant DNA Re-methylation Improves Post-implantation Development of Somatic Cell Nuclear Transfer Embryos

Rui Gao,[1,2] Chenfei Wang,[1,2] Yawei Gao,[1,2] Wenchao Xiu,[1] Jiayu Chen,[1] Xiaochen Kou,[1] Yanhong Zhao,[1] Yuhan Liao,[1] Dandan Bai,[1] Zhibin Qiao,[1] Lei Yang,[1] Mingzhu Wang,[1] Ruge Zang,[1] Xiaoyu Liu,[1] Yanping Jia,[1] Yanhe Li,[1] Yalin Zhang,[1] Jiqing Yin,[1] Hong Wang,[1] Xiaoping Wan,[1] Wenqiang Liu,[1,*] Yong Zhang,[1,*] and Shaorong Gao[1,3,*]

[1]Clinical and Translational Research Center of Shanghai First Maternity and Infant Hospital, Shanghai Key Laboratory of Signaling and Disease Research, School of Life Sciences and Technology, Tongji University, Shanghai 200092, China

[2]These authors contributed equally

[3]Lead Contact

*Correspondence: liuwenqiang@tongji.edu.cn (W.L.), yzhang@tongji.edu.cn (Y.Z.), gaoshaorong@tongji.edu.cn (S.G.)

https://doi.org/10.1016/j.stem.2018.07.017

SUMMARY

Somatic cell nuclear transfer (SCNT) enables cloning of differentiated cells by reprogramming their nuclei to a totipotent state. However, successful full-term development of SCNT embryos is a low-efficiency process and arrested embryos frequently exhibit epigenetic abnormalities. Here, we generated genome-wide DNA methylation maps from mouse pre-implantation SCNT embryos. We identified widespread regions that were aberrantly re-methylated, leading to mis-expression of genes and retrotransposons important for zygotic genome activation. Inhibition of DNA methyltransferases (Dnmts) specifically rescued these re-methylation defects and improved the developmental capacity of cloned embryos. Moreover, combining inhibition of Dnmts with overexpression of histone demethylases led to stronger reductions in inappropriate DNA methylation and synergistic enhancement of full-term SCNT embryo development. These findings show that excessive DNA re-methylation is a potent barrier that limits full-term development of SCNT embryos and that removing multiple epigenetic barriers is a promising approach to achieve higher cloning efficiency.

INTRODUCTION

Somatic cell nuclear transfer (SCNT) enables the genome of a somatic cell to be reprogrammed into a totipotent state, which allows the generation of both cloned animals and nuclear transfer embryonic stem cells (ntESCs) (Chung et al., 2014; Liu et al., 2018; Tachibana et al., 2013; Wakayama et al., 1998; Wilmut et al., 1997). Thus, the SCNT technique holds great promise for animal husbandry and human therapeutic cloning. However, the efficiency of complete nuclear reprogramming via SCNT is extremely low in terms of blastocyst development and production of full-term animals (Yang et al., 2007). Many abnormalities in cloned embryos have been observed, including unfaithful DNA demethylation, impaired histone modifications, and incomplete zygotic genome activation (ZGA) (Teperek and Miyamoto, 2013). Therefore, incomplete epigenetic reprogramming of the somatic cell genome has been suggested as the major cause for inefficient SCNT-mediated reprogramming.

High levels of DNA methylation in cloned embryos have been observed across species, and aberrant DNA methylation patterns can be detected even after implantation (Dean et al., 2001; Peat and Reik, 2012; Teperek and Miyamoto, 2013). Previously, an inverse correlation was found between aberrant DNA methylation and developmental potential (Dean et al., 2003; Wei et al., 2011). Reduced representation bisulfite sequencing (RRBS) has been performed using late 1-cell-stage SCNT embryos, and more than 20 genes, along with long interspersed elements (LINEs) and long terminal repeats (LTRs), were defined as demethylation-resistant regions (Chan et al., 2012). In addition to DNA methylation, abnormal histone modifications have also been reported in cloned embryos (Hörmanseder et al., 2017; Liu et al., 2016; Matoba et al., 2014; Wang et al., 2007). High levels of methylation on H3K9 have been found to inhibit the re-activation of genes in 2-cell embryos, and removal of H3K9me3 was shown to markedly improve cloning efficiency (Antony et al., 2013; Liu et al., 2016; Matoba et al., 2014). Moreover, H3K4 methylation imposes an inappropriate active transcriptional state of donor-cell-specific genes, and reduced H3K4 methylation can substantially improve transcriptional reprogramming of cloned embryos (Hörmanseder et al., 2017).

Many advances have been made in SCNT technology via different epigenetic approaches, such as increasing histone acetylation levels in the reconstructed embryos by deacetylase inhibitors, reducing H3K9 and H3K4 methylation levels in SCNT embryos, correcting *Xist* gene expression levels in cloned embryos, and reducing the DNA methylation levels of donor cells (Hörmanseder et al., 2017; Inoue et al., 2010; Kishigami et al., 2006a; Matoba et al., 2011, 2014; Van Thuan et al., 2009). By combining embryo biopsy system and single-cell RNA sequencing (RNA-seq) profiles, our recent study analyzed cloned embryos with different development potencies and improved SCNT blastocyst development to over 95%, comparable to

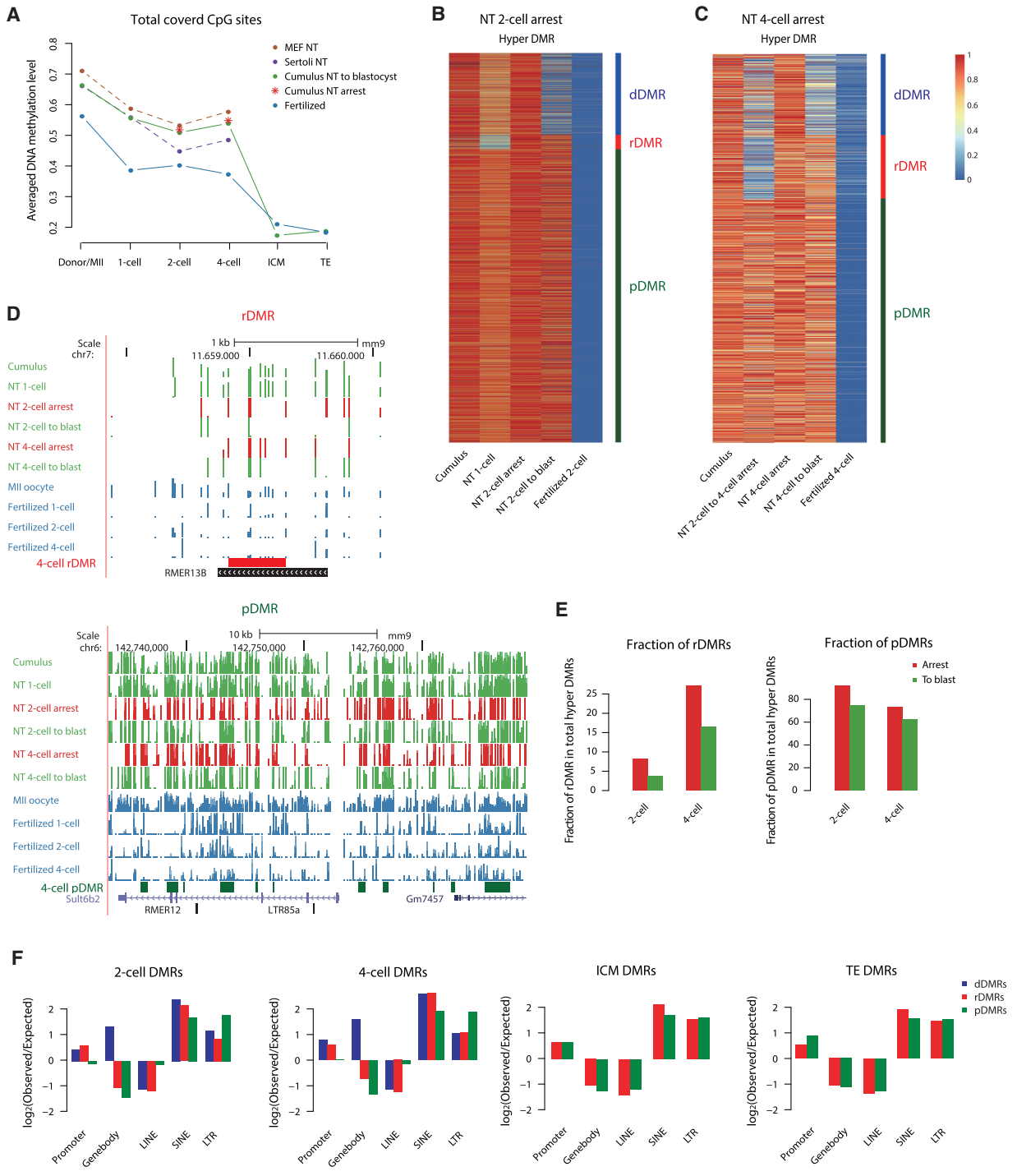

Figure 1. Aberrant DNA Re-methylation Occurs in SCNT Embryos

(A) Global DNA methylation levels during NT and fertilized embryo development. Each dot represents the averaged CpG methylation level. ICM, inner cell mass; MEF, mouse embryonic fibroblast; TE, trophectoderm.

(B) Heatmap showing hyper-DMRs between NT 2-cell arrest and fertilized 2-cell samples. Each row represents a 300-bp genomic window of hyper-DMRs, and colors represent averaged CpG methylation levels. DMRs are classified into three categories: dDMR; rDMR; and pDMR; see STAR Methods.

(C) Heatmap showing hyper-DMRs between NT 4-cell arrest and fertilized 4-cell samples.

(D) University of California, Santa Cruz (UCSC) genome browser view of representative rDMRs near RMER13B locus (upper) and a cluster of pDMRs (lower). Signal represents DNA methylation level.

(legend continued on next page)

that of fertilized embryos (Liu et al., 2016). However, SCNT efficiency for producing cloned animals still remains low (Liu et al., 2016; Matoba et al., 2014), indicating that the poor success rate for cloned offspring production following histone resetting, as compared to fertilized embryos, may arise from other reprogramming barriers, such as DNA methylation.

In the present study, we combined the embryo biopsy system and ultra-low-input whole-genome bisulfite sequencing (WGBS) technology to validate and emphasize the role of DNA methylation in SCNT embryos. We observed abnormally high levels of DNA methylation in SCNT embryos. In particular, we identified widespread regions that were aberrantly re-methylated, leading to unfaithful activation of genes and retrotransposons in SCNT embryos. Removal of DNA re-methylation through interference of *de novo* Dnmts could re-activate specific subsets of SCNT transcriptome and evidently improve the developmental potential. Inactivation of Dnmts combined with overexpression of histone demethylases further reduced the global hyper-methylation status in SCNT embryos and led to a synergistic enhancement effect on the full-term development of nuclear transfer embryos. Overall, our study demonstrated that the re-methylation memory inherited from donor cells acts as a critical epigenetic barrier for SCNT embryo development and that overcoming multiple epigenetic barriers would be a promising approach to generate cloned animals efficiently.

RESULTS

Global Hyper DNA Methylation Patterns in SCNT Embryos

A large fraction of SCNT embryos are arrested at early cleavage stages. Although evidence has shown links between abnormal DNA methylation patterns and the poor developmental potential of embryos, the genome-wide DNA methylation maps of pre-implanted SCNT embryos remain undetermined. To precisely dissect the DNA methylation changes among SCNT embryos with distinct developmental potentials, we combined the embryo biopsy system and ultra-low-input WGBS technology to generate a genome-wide, single-base-pair-resolution map of DNA methylation from SCNT-reconstructed mouse embryos in early developmental stages (Figure S1A). Pre-implantation developmental potency of cloned embryos was previously reported to be unaffected by blastomere biopsy (Liu et al., 2016). Hence, we obtained three types of cloned embryos in the 2-cell embryo biopsy system: SCNT embryos arrested at the 2-cell stage (NT 2-cell arrest); SCNT embryos arrested at the 4-cell stage (NT 2-cell to 4-cell arrest); and SCNT embryos that developed into blastocysts (NT 2-cell to blast; Figure S1A). In the 4-cell embryo biopsy system, we obtained two types of samples: SCNT embryos arrested at the 4-cell stage (NT 4-cell arrest) and SCNT embryos that developed into blastocysts (NT 4-cell to blast; Figure S1A). Donor cumulus cells (CCs) and fertilized embryos (from 1-cell to blastocyst stage) were analyzed as control samples.

We generated ultra-low-input WGBS data of SCNT embryos from donor cumulus cells to blastocyst stage (Figure S1B; Table S1), and WGBS data of the fertilized embryos were from our previous study (Wang et al., 2018). After comparing the dynamics of DNA methylation from donor cells to the 4-cell stage, we found that the global DNA methylation levels in SCNT embryos were much higher than fertilized embryos (Figure 1A). Moreover, relatively higher DNA methylation levels can be detected in developmentally arrested SCNT embryos at the 2- and 4-cell stages compared to those that had proceeded to blastocysts (Figure 1A). These results suggest that incomplete DNA de-methylation might have a close relationship with developmental arrest of SCNT embryos. The overall DNA methylation level between SCNT and fertilized embryos become comparable at the blastocyst stage; however, we can still identify thousands of aberrant gain and loss of regions in the inner cell mass (ICM) and trophectoderm (TE) samples, which might contribute to the low success rate of SCNT after implantation (Figure S1C). Above all, our data indicated that impaired DNA methylation might be an unavoidable barrier in pre-implantation SCNT embryos.

Aberrant DNA Re-methylation Occurs in SCNT Embryos

In contrast to the normal fertilized development process (Wang et al., 2014, 2018), the 4-cell SCNT samples exhibited unusual increased methylation levels compared with the 2-cell embryos (Figure 1A). To further explore the underlying molecular mechanism of this unique pattern in SCNT embryos, we identified differentially methylated regions (DMRs) between SCNT embryos and fertilized controls (Figure S1C). We initially compared arrested SCNT embryos to fertilized embryos and focused on the hyper-DMRs at the 2- and 4-cell stages (Figures 1B and 1C). Consistent with previous studies, a fraction of regions in NT to blastocyst samples were de-methylated to similar degrees compared with fertilized embryos, which we defined as de-methylated DMRs (dDMRs) (Figures 1B and 1C). However, the majority of the hyper-methylated regions in NT-arrested embryos, which might be inherited from the donor cells, still maintained high methylation levels in NT to blastocyst samples, and these regions were defined as persistently methylated DMRs (pDMRs) (Figures 1B–1D). Intriguingly, we found that a significant proportion of DMRs possessed higher methylation level than their former developmental stage, indicating that these regions are re-methylated during SCNT embryo development, and we defined these regions as re-methylated DMRs (rDMRs) (Figures 1B–1D). Unlike pDMRs, which are moderately similar in NT arrest and NT to blastocyst samples, the NT arrest samples possessed almost twice as many rDMRs as NT to blastocyst samples (Figure 1E). These results indicate that the re-methylation process might be tightly correlated with unfaithful SCNT embryogenesis at the 2-cell and 4-cell stages. Moreover, pDMRs were more frequently inherited from cleaved embryos to blastocyst stage, which reflects their functional irrelevance in the arrest of SCNT embryos (Figure S1D). Collectively, these results raise the possibility that rDMRs in SCNT embryos genome function as an

(E) Barplots showing the fractions of rDMRs and pDMRs in total hyper-DMRs between NT arrest and NT to blast samples.
(F) Barplots showing the enrichment of 2-cell and 4-cell dDMRs, rDMRs, and pDMRs as well as ICM and TE rDMRs and pDMRs in genomic regions of SCNT embryos. The y axis represents log2 observed versus expected number of DMRs in each category; see STAR Methods.
See also Figure S1 and Table S1.

evident barrier, whose proper removal can rescue the developmental arrest at cleavage stages and facilitate proceeding to blastocyst development.

In addition, we found that rDMRs were specifically enriched at promoters in SCNT-cleaved embryos, which might be partially responsible for the transcriptome defects in cleavage stage (Figures 1F and S1E). Besides, both rDMRs and pDMRs were largely enriched at short interspersed elements (SINEs) and LTRs instead of LINEs in all analyzed SCNT embryos, which was different from previous reported de-methylation resistance of LINE and LTR elements using RRBS data (Figures 1F and S1E; Chan et al., 2012).

As the paternal zygotic genome derived from immature spermatozoa was reported to be highly re-methylated before first mitosis after demethylation (Kishigami et al., 2006b), we then asked whether the re-methylation memory in cloned embryos might also be inherited from donor cells. Hence, we used more donor cell types, including sertoli cells (SCs) and mouse embryonic fibroblasts (MEFs), to analyze the extensive methylome reprogramming in reconstructed SCNT embryos. Notably, aberrant DNA re-methylation generally occurs at 2-cell and 4-cell stage in SCNT embryos derived from overall different donor cells, suggesting its common feature during SCNT-mediated reprogramming (Figure 1A). In addition, we found that rDMRs display great cell type specificity and pDMRs are more conserved (Figure S1F), indicating that rDMRs arise possibly due to the cell-type-specific memory of Dnmt3a and/or Dnmt3b binding (Velasco et al., 2010; Figure S1G). The above results suggest that a dynamic equilibrium of re-methylation, persistent methylation, and de-methylation occurs in pre-implantation SCNT embryos and that it is critical to verify the effect of re-methylation when referring to the developmental potential of cloned embryos.

Hyper-methylation of SCNT Embryos Causes Transcriptome Disorders

To further investigate how insufficient epigenetic reprogramming affects gene re-activation in SCNT embryos, we performed a comprehensive analysis of the transcriptome and DNA methylome data from SCNT embryos. Initially, we performed an unbiased, unsupervised weighted gene co-expression network analysis (WGCNA) (Langfelder and Horvath, 2008) and found that the transcriptomes of SCNT embryos were clearly defective compared with fertilized embryos, especially at the 4-cell and blastocyst stages (Figures S2A and S2B). To evaluate the influence of aberrant DNA methylation levels on embryonic gene expression, we first defined the DNA-methylation-affected genes by comparing the changes in expression and DNA methylation levels between NT arrest and fertilized embryos (Figure 2A). As expected, we can identify a subset of methylation-affected genes with either repressed (n = 197 in 2-cell and n = 302 in 4-cell) or activated (n = 227 in 2-cell and n = 115 in 4-cell) status in SCNT embryos (Figure 2A). Functional analysis of these genes revealed that they were largely enriched in biological processes required for normal embryo development (Figure S2C). In addition, we found that the methylation-affected downregulated genes were highly enriched for totipotent- and developmental-related genes (Figures 2B and S2D), which might be vital for proper ZGA and establishing totipotency at 2-cell stage. Notably, among all these methylation-affected downregulated genes, only rDMR specifically affected ones were significantly de-methylated and re-activated in NT to blastocyst embryos (Figures 2C and S2E). These results demonstrated that aberrant DNA hyper-methylation, especially re-methylation, could affect the development potency of cleaved SCNT embryos through regulating crucial totipotent and developmental genes.

A large fraction of retro-transposons are believed to become hypo-methylated and activated during early ZGA (Peaston et al., 2004). We further explored how DNA methylation contributes to the regulation of retro-transposons during SCNT embryo development. In contrast with the gene expression profiles, we only defined a subgroup of downregulated retro-transposons accompanied by aberrant hyper-DNA methylation status in the 2- and 4-cell stages, reflecting that the highly restrained expression of repeat elements is possibly due to their hyper-DNA methylation (Figure 2D). Moreover, these downregulated retro-transposons maintained their high methylation and low expression levels in NT to blastocyst samples (Figures S2E and S2F). For instance, unlike genome-wide demethylation of retro-transposons in fertilized embryos, the MERVL elements exhibited a dramatically higher remnant methylation state in SCNT embryos than in fertilized embryos, and its transcription activity was evidently repressed (Figure 2E). These data indicated that certain retro-transposons were more likely to be refractory to de-methylation and might be protected within the epigenetic context of somatic cells in cloned embryos.

Reduced DNA Re-methylation Improves the Development of SCNT Embryos

Having established a correlation between the imperfect re-methylation and developmental failure of SCNT embryos, we next asked whether blockade of re-methylation could improve the poor development of cloned animals. Hence, enucleated recipient MII oocytes were injected with short interfering RNAs (siRNAs) targeting DNA cytosine methyltransferases, *Dnmt3a* and *Dnmt3b*, to inactivate the function of *de novo* DNA re-methylation (Figure S3A). We found that the averaged methylation level of SCNT embryos could be reduced by inhibition of Dnmts alone (Figures 3A and S3B; Table S1), although still higher than fertilized embryos at the same developmental stage. We then addressed the effects of Dnmts on genome-wide re-methylation patterns during early cloned development. Knockdown of *Dnmt3a* and *Dnmt3b* was more likely to alleviate fractions of re-methylated regions in cloned embryos, and the persistently methylated loci showed moderate changes compared with NT to blastocyst samples (Figure 3B). Moreover, inactivation of Dnmts could clearly restore the expression levels of most rDMR-affected genes and retro-transposons, accompanied by the loss of DNA methylation marks in cleaved SCNT embryos (Figures 3C and S3C). These re-activated factors were largely decision marks of totipotency and development, including MERVLs (Figure 3D). Taken together, these data indicated that interference of Dnmts could restore the expression levels of certain genes and retro-transposons directly through reducing DNA re-methylation in cleaved SCNT embryos.

On the basis of the above results, we further analyzed the developmental capacity of SCNT embryos derived from cumulus cells, which were treated by inactivation of Dnmts alone. The

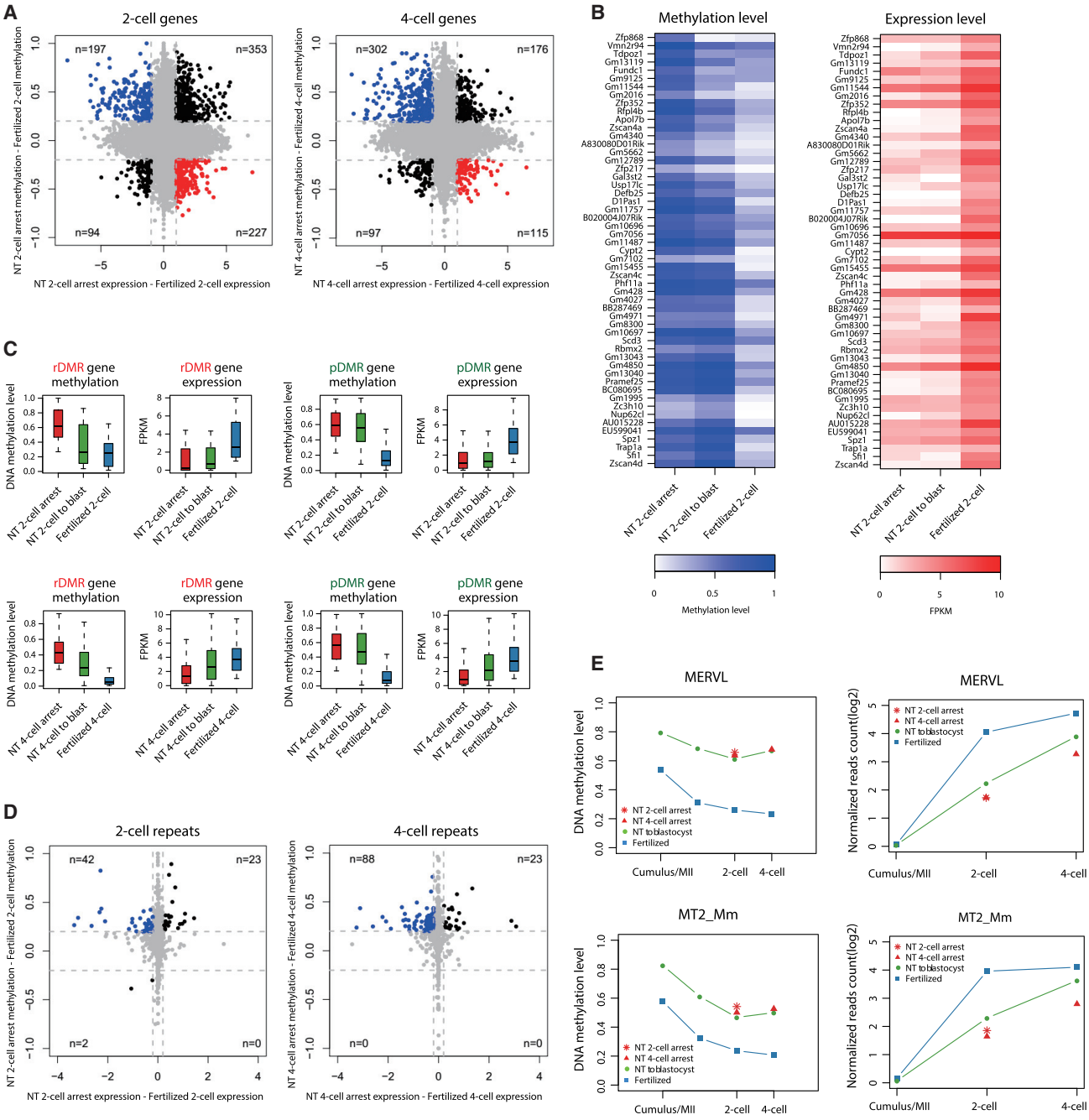

Figure 2. Hyper-methylation of SCNT Embryos Leads to Dysregulated Transcriptional Activities

(A) Scatterplots showing the comparison between the transcriptome and the DNA methylome at the 2-cell (left) and 4-cell (right) stages at the gene level. Genes with significant changes in DNA methylation levels (abs change > 0.2) and expression levels (abs change > 1) are defined as "methylation-affected genes" and labeled in different colors. Methylation-affected downregulated genes are labeled in blue; methylation-affected upregulated genes are labeled in red.

(B) Heatmaps showing the DNA methylation levels (left) and expression levels (right) of 53 2-cell embryo specifically expressed genes.

(C) Boxplots showing the DNA methylation and expression levels of the methylation-affected downregulated genes (blue dots in Figure 2A) at the 2-cell and 4-cell stages. rDMR- and pDMR-affected genes are defined based on the re-methylation status compared to the prior developmental stage, see STAR Methods.

(D) Scatterplots showing the comparison between the transcriptome and the DNA methylome at the 2-cell (left) and 4-cell (right) stages at the repeat level. Repeats with significant changes in DNA methylation level (abs change > 0.2) and expression level (abs change > 0.2) are defined as "methylation-affected repeats" and labeled in different colors. Methylation-affected downregulated repeats are labeled in blue. No methylation-affected upregulated repeats are identified at 2-cell and 4-cell stages.

(E) Averaged DNA methylation levels (left) and expression levels (right) of the repeat class MERVLs (MERVL and MT2_Mm) during NT and fertilized embryo development.

See also Figure S2.

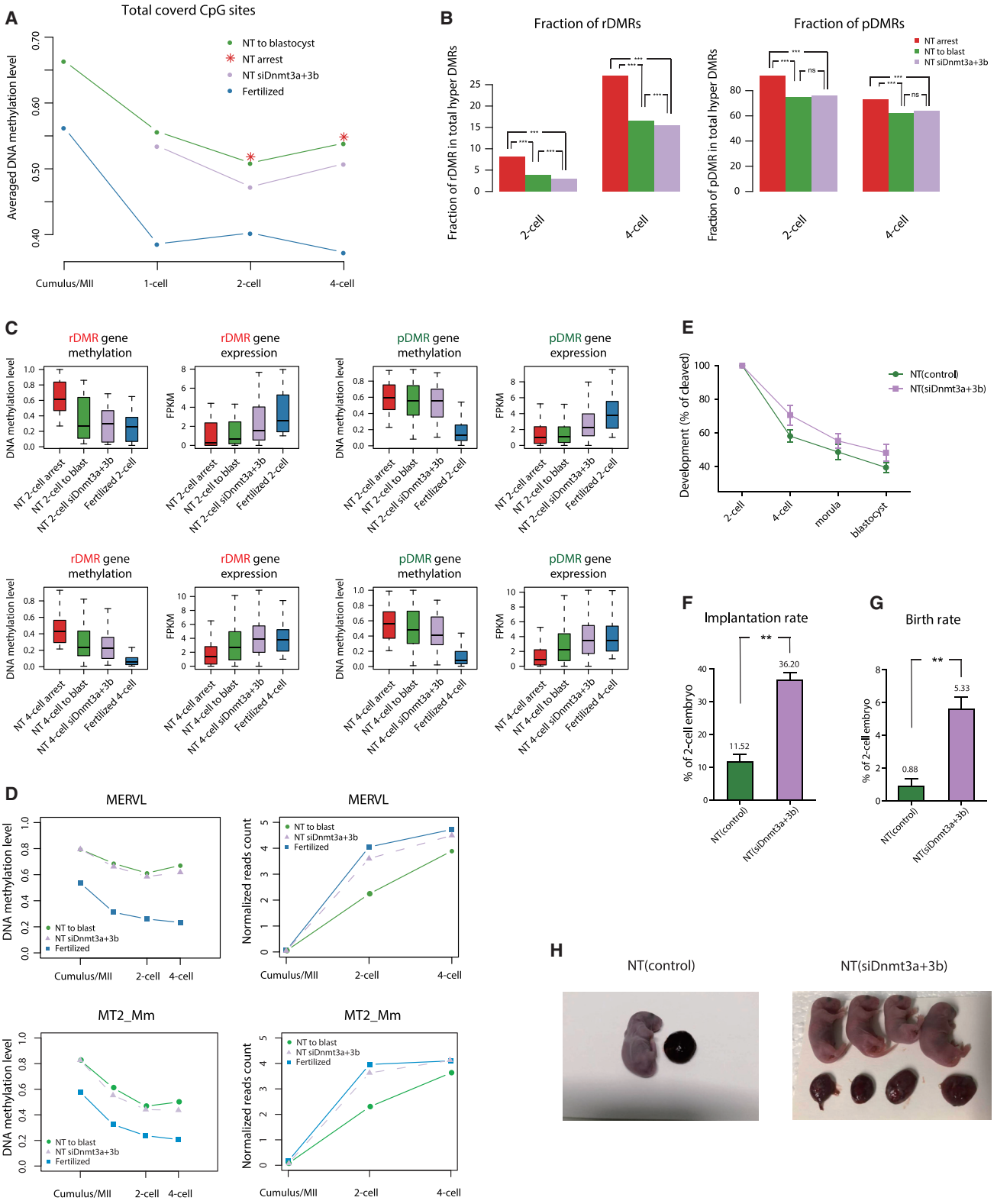

Figure 3. Knockdown of Dnmts Alleviates DNA Re-methylation and Improves the Development of SCNT Embryos

(A) Global DNA methylation levels during NT arrest, NT to blastocyst, NT siDnmt3a+3b, and fertilized embryo development. Each dot represents the averaged CpG methylation level.

(legend continued on next page)

blastocyst development of NT(siDnmt3a+3b) embryos was nearly 10% higher than uninjected control embryos (48.2% versus 39.5%; Figures 3E and S3D; Table S3). Moreover, caesarian section at embryonic day 19.5 (E19.5) (the day of term) revealed that the rate of implantation, evidenced by implantation sites, was 3-fold higher in NT(siDnmt3a+3b) embryos (36.2%) than in control SCNT embryos (11.5%; Figure 3F; Table S4). Importantly, 5.33% of transferred siDnmt3a+3b-injected 2-cell SCNT embryos developed to term, and only 0.88% of the transferred control embryos developed to term under the same conditions (Figures 3G and 3H; Table S4). Further to our surprise, we observed that inhibition of Dnmts in cloned embryos could contribute to smaller placentae compared to control SCNT embryos (0.24 g versus 0.39 g; Figures 3H and S3E; Table S4), whereas the body weight of NT(siDnmt3a+3b) fetus showed little difference from the uninjected cloned pups (Figures 3H and S3E; Table S4). Besides, knocking down Dnmts led to less placental abnormalities in cloned embryos, including a higher degree of vascularization, more integrate trophoblastic epithelium, and a thinner subtrophoblastic basement membrane (Figure S3F). Therefore, we concluded that DNA re-methylation acts as a barrier during SCNT-mediated reprogramming and that its removal by interference of *de novo* DNA cytosine methyltransferases could evidently improve the developmental potential of SCNT embryos.

Combined DNA and Histone Modifier Treatments Achieve Higher Cloning Efficiency

Protein partners have been previously identified for the Dnmts, including histone deacetylases, histone methyltransferases, and transcription factors (Freitag and Selker, 2005), and our recent work has also demonstrated that the averaged methylation level of SCNT embryos could be partially rescued by co-injection of two key histone regulators, *Kdm4b* and *Kdm5b* (Liu et al., 2016). We thus sought to investigate the effect of combining DNA and histone modifier treatments on loss of the aberrant DNA methylation marks (Table S1). Kdm4b+5b mRNA and Dnmt3a+3b siRNA co-injected, rather than siDnmt3a+3b only, SCNT embryos exhibited methylation levels that were more comparable to those of fertilized embryos at each developmental stage (Figures 4A and S4A). Importantly, we found that the combinational strategy could significantly reduce the methylation level on both rDMRs and pDMRs, suggesting a synergistic enhancement influence of multiple epigenetic configurations on reducing the hyper-DNA methylation statue of SCNT embryos (Figure 4B). Moreover, combinational strategy synergistically restored the methylation-affected transcriptome to re-activation, accompanied by further loss of methylation marks compared to blockade of Dnmts alone (Figures 4C and S4B). For example, MERVL elements exhibited decreased methylation levels and increased expression levels in 2- and 4-cell SCNT embryos upon co-injection of Kdm4b+5b mRNA and Dnmt3a+3b siRNA, as compared to single treatment (Figure S4C). These data indicated that combinational strategy could further rescue the aberrant RNA expression profiles through more sufficient DNA de-methylation.

Finally, we investigated whether combined DNA and histone modifier treatments could further enhance the poor cloning efficiency, using cumulus cells as donors. Almost all NT(siDnmt3a+3b&oeKdm4b+5b) embryos developed to blastocyst stage, with even higher rate than NT(oeKdm4b+5b) embryos (Figures S4D and S4E; Table S3). Additionally, the implantation rate and full-term development of NT(siDnmt3a+3b&oeKdm4b+5b) embryos were evidently increased compared to either single-strategy-treated SCNT embryos or untreated control SCNT embryos (Figures 4D and S4F; Table S4). Intriguingly, we observed that only knocking down Dnmts could contribute to smaller placentae in SCNT embryos, and overexpressing histone demethylases showed little corrective affluence on placental abnormalities (Figure S4G; Table S4), which suggested that the "DNA re-methylation barrier" might be independent, as compared to the "histone barriers" during SCNT-mediated reprogramming. Above all, these observations demonstrated an important issue regarding the synergistic effects of DNA and histone modifiers on the success of SCNT, indicating that combinational treatments of multiple epigenetic regulators might be a most promising approach to achieve higher cloning efficiency.

DISCUSSION

Despite the tremendous application potential of SCNT technology, cloning efficiency still remains low in most species, and the mechanism underlying epigenetic reprogramming following SCNT remains largely undefined (Teperek and Miyamoto, 2013). In this study, we observed an unexpected *de novo* DNA re-methylation during SCNT pre-implantation embryogenesis, which leads to unfaithful activation of genes and retro-transposons and constitutes an essential cause for the poor development of cloned embryos. In addition to rodent cloned embryos, this unique DNA re-methylation pattern has also been considered as a conserved regulatory feature during early primate development (Gao et al., 2017; Zhu et al., 2018). Moreover, previous work that embryos formed from immature spermatozoa

(B) Barplots showing the fractions of rDMRs (left) and pDMRs (right) in total hyper-DMRs in NT arrest, NT to blast, and NT siDnmt3a+3b embryos at 2-cell and 4-cell stages. Significance between different treatment groups were evaluated using Fisher's exact test; *** represents p value < 2.2E−16; ns represents p value > 0.05.

(C) Boxplots showing the DNA methylation and expression levels of the methylation-affected downregulated genes (blue dots in Figure 2A) at the 2-cell and 4-cell stages.

(D) Averaged DNA methylation levels (left) and expression levels (right) of the repeat class MERVLs (MERVL and MT2_Mm) during NT, NT siDnmt3a+3b, and fertilized embryo development.

(E) The pre-implantation development of SCNT embryos derived from cumulus cells followed until the blastocyst stage. Shown is the percentage of embryos that reach each indicated stage.

(F and G) Implantation rate (F) and birth rate (G) of SCNT embryos derived from cumulus cells examined by caesarian section on E19.5.

(H) Representative images of fetuses produced from NT(siDnmt3a+3b) and uninjected control NT embryos, both derived from cumulus cells.

Data in (F) and (G) are represented as mean ± SEM. **p < 0.01 by Student's t test for comparison. See also Figure S3 and Tables S1, S3, and S4.

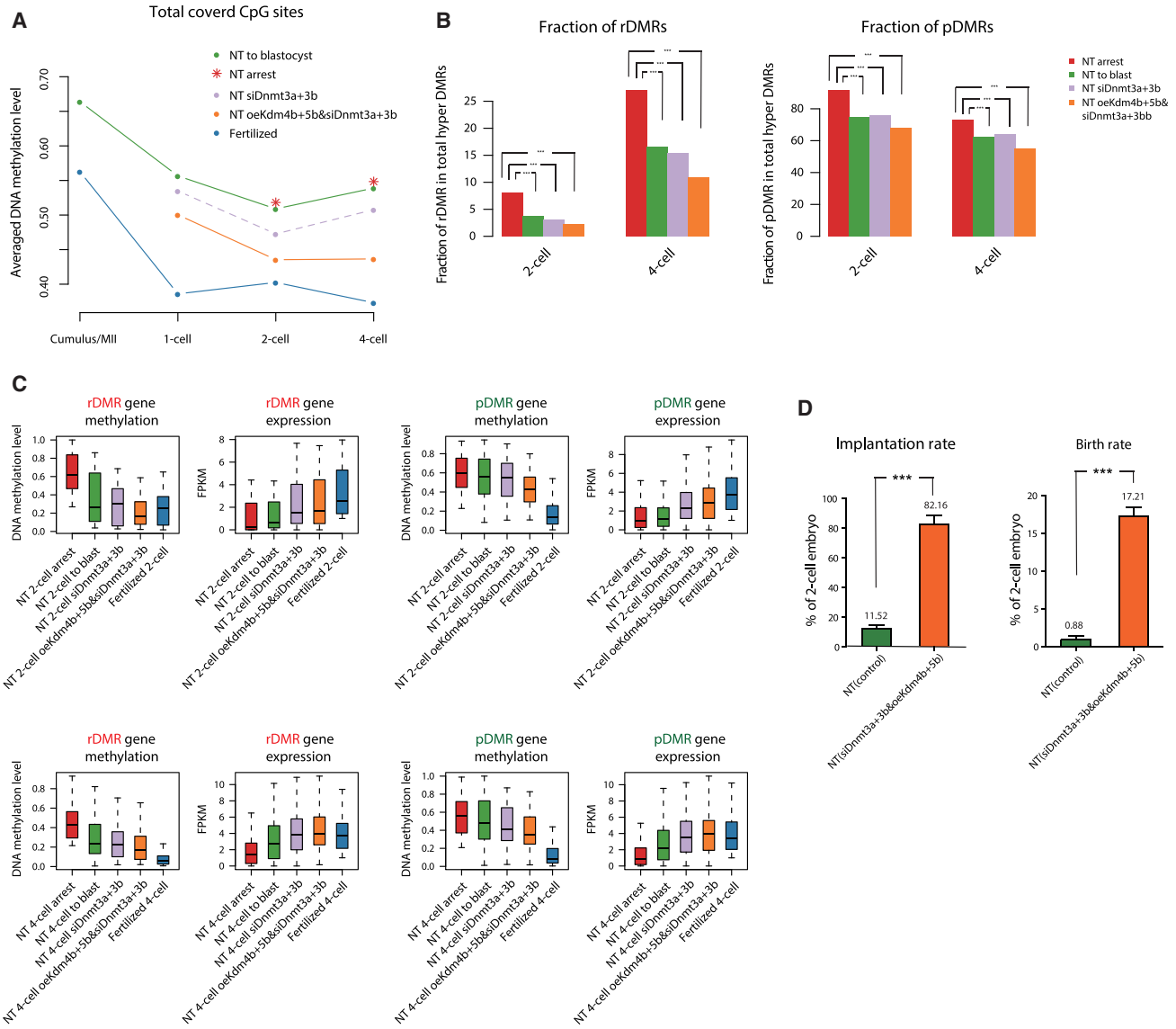

Figure 4. Combined Approaches Achieve Higher Cloning Efficiency

(A) Global DNA methylation levels during NT arrest, NT to blastocyst, NT siDnmt3a+3b, NT siDnmt3a+3b&oeKdm4b+5b, and fertilized embryo development. Each dot represents the averaged CpG methylation level.

(B) Barplots showing the fractions of rDMRs (left) and pDMRs (right) in total hyper-DMRs in NT arrest, NT to blast, NT siDnmt3a+3b, and NT siDnmt 3a+3b&oeKdm4b+5b embryos at 2-cell and 4-cell stages. Significance between different treatment groups was evaluated using Fisher's exact test; *** represents p value < 2.2E−16.

(C) Boxplots showing the DNA methylation and expression levels of the methylation-affected downregulated genes (blue dots in Figure 2A) at the 2-cell and 4-cell stages.

(D) Implantation rate and birth rate of SCNT embryos derived from cumulus cells examined by caesarian section on E19.5. Data are represented as mean ± SEM. ***p < 0.001 by Student's t test for comparison.

See also Figure S4 and Tables S1, S3, and S4.

develops with aberrant genome-wide DNA re-methylation in their paternal genomes (Kishigami et al., 2006b). These observations collectively suggested that the impact of transgenerational re-methylation memory from gametes or donor cells should be considered when investigating the epigenetic reprogramming of offspring.

Oocytes can reprogram a terminally differentiated cell into a totipotent embryo, with the capacity to generate an entire organism. 2-cell totipotent cells are generally characterized by the activation of endogenous retroviral elements (ERVs), MERVL elements, and 2C-specific genes (Eckersley-Maslin et al., 2016; Falco et al., 2007; Macfarlan et al., 2012). Our findings showed that rDMRs and pDMRs are largely enriched at LTR elements, which also supported our hypothesis that aberrant DNA methylation status at the 2-cell stage may account for the failed establishment of totipotency in SCNT embryos (Wang and Dey, 2006).

Numerous previous works have suggested that multiple epigenetic modifications may interrupt SCNT reprogramming (Matoba and Zhang, 2018). However, a clear picture is still lacking on the cross-talk among those epigenetic configurations during the nuclear reprogramming via SCNT. With our data, we found that knocking down Dnmts was more likely to alleviate fractions of re-methylated regions in cloned embryos, although the persistently methylated loci showed moderate changes, whereas combinational histone demethylases strategy markedly alleviated the fraction of persistent methylation. This result raised an important issue, suggesting that each reprogramming process may require a sequential coordination of multiple epigenetic features. Consistently, recent work has shown that loss of H3K27me3-dependent imprinting inhibits post-implantation development of cloned embryos, even after other roadblocks such as H3K9me3 and ectopic X chromosome inactivation have been overcome (Matoba et al., 2018).Further work is needed to validate and emphasize the roles of hierarchical epigenetic rearrangements in other reprogramming processes.

In conclusion, our study demonstrated that incomplete DNA methylation reprogramming, especially DNA re-methylation, disrupted the developmental potential of cloned embryos. Knockdown of Dnmts facilitated the activation of totipotent genes and retro-transposons, thus providing a positive correlation between rectified DNA methylation reprogramming and improved developmental competence of cloned embryos.

STAR★METHODS

Detailed methods are provided in the online version of this paper and include the following:

- KEY RESOURCES TABLE
- CONTACT FOR REAGENT AND RESOURCE SHARING
- EXPERIMENTAL MODEL AND SUBJECT DETAILS
  - Mice
  - Donor cell preparation
- METHOD DETAILS
  - Somatic cell nuclear transfer and embryo culture
  - *In vitro* transcription of mRNA and direct injection
  - Knockdown of Dnmt3a/3b in cloned embryo
  - Reverse transcription and quantitative RT-PCR analysis
  - Embryo transfer
  - Biopsy culture system
  - WGBS library preparation
  - Generation of RNA-Seq library
- QUANTIFICATION AND STATISTICAL ANALYSIS
  - Biological replicates
  - Statistical analysis
  - Mapping and quantification of RNA-seq and WGBS data
  - Expression and methylation level quantification of repeats elements
  - DMR calling and classification
  - Donor-specific DMR definition
  - Genomic annotations and enrichment calculation
  - WGCNA analysis
  - Consistency analysis between DNA methylation and gene expression
  - Gene ontology analysis
- DATA AND SOFTWARE AVAILABILITY

SUPPLEMENTAL INFORMATION

Supplemental Information includes four figures and four tables and can be found with this article online at https://doi.org/10.1016/j.stem.2018.07.017.

ACKNOWLEDGMENTS

We are grateful to our colleagues in the laboratory for their assistance with the experiments and in the preparation of this manuscript. We thank Dr. Zefeng Wang and the PICB Bio-Med Big Data Center for providing computational platforms. This work was primarily supported by the National Key R&D Program of China (2016YFA0100400) and the National Natural Science Foundation of China (31721003). This work was also supported by the Ministry of Science and Technology of China (2017YFA0102602, 2018YFA0108900, 2015CB964800, 2015CB964503 and 2017YFA0103300), the National Natural Science Foundation of China (81630035, 31771646, 31501196, and 31430056), the Shanghai Subject Chief Scientist Program (15XD1503500), the Shanghai Rising-Star Program (17QA1402700 and 17QA1404200), the Shanghai Chenguang Program (16CG17, 16CG19, and 14CG16), the Shanghai municipal medical and health discipline construction projects (2017ZZ02015), National Postdoctoral Program for Innovative Talents (BX201700307 and BX20170174), China Postdoctoral Science Foundation (2017M621527), and the Fundamental Research Funds for the Central Universities (1515219049).

AUTHOR CONTRIBUTIONS

W.L., Yong Zhang, and S.G. conceived and designed the experiments. R.G. and W.L. performed most of the experiments. C.W. and W.X. performed the computational analysis. R.G., C.W., and Y.G. designed and performed the data analysis. J.C., X.K., Y. Zhao, Y. Liao, D.B., Z.Q., L.Y., M.W., R.Z., X.L., Y.J., Y. Li, Yalin Zhang, J.Y., and H.W. assisted with the sample and library preparation. R.G., C.W., W.L., Yong Zhang, and S.G. wrote the manuscript.

DECLARATION OF INTERESTS

The authors declare no competing interests.

Received: January 16, 2018
Revised: June 26, 2018
Accepted: July 30, 2018
Published: August 23, 2018

REFERENCES

Antony, J., Oback, F., Chamley, L.W., Oback, B., and Laible, G. (2013). Transient JMJD2B-mediated reduction of H3K9me3 levels improves reprogramming of embryonic stem cells into cloned embryos. Mol. Cell. Biol. *33*, 974–983.

Chan, M.M., Smith, Z.D., Egli, D., Regev, A., and Meissner, A. (2012). Mouse ooplasm confers context-specific reprogramming capacity. Nat. Genet. *44*, 978–980.

Chung, Y.G., Eum, J.H., Lee, J.E., Shim, S.H., Sepilian, V., Hong, S.W., Lee, Y., Treff, N.R., Choi, Y.H., Kimbrel, E.A., et al. (2014). Human somatic cell nuclear transfer using adult cells. Cell Stem Cell *14*, 777–780.

Dean, W., Santos, F., Stojkovic, M., Zakhartchenko, V., Walter, J., Wolf, E., and Reik, W. (2001). Conservation of methylation reprogramming in mammalian development: aberrant reprogramming in cloned embryos. Proc. Natl. Acad. Sci. USA *98*, 13734–13738.

Dean, W., Santos, F., and Reik, W. (2003). Epigenetic reprogramming in early mammalian development and following somatic nuclear transfer. Semin. Cell Dev. Biol. *14*, 93–100.

Dobin, A., Davis, C.A., Schlesinger, F., Drenkow, J., Zaleski, C., Jha, S., Batut, P., Chaisson, M., and Gingeras, T.R. (2013). STAR: ultrafast universal RNA-seq aligner. Bioinformatics *29*, 15–21.

Eckersley-Maslin, M.A., Svensson, V., Krueger, C., Stubbs, T.M., Giehr, P., Krueger, F., Miragaia, R.J., Kyriakopoulos, C., Berrens, R.V., Milagre, I., et al. (2016). MERVL/Zscan4 network activation results in transient genome-wide DNA demethylation of mESCs. Cell Rep. *17*, 179–192.

Falco, G., Lee, S.L., Stanghellini, I., Bassey, U.C., Hamatani, T., and Ko, M.S.H. (2007). Zscan4: a novel gene expressed exclusively in late 2-cell embryos and embryonic stem cells. Dev. Biol. *307*, 539–550.

Freitag, M., and Selker, E.U. (2005). Controlling DNA methylation: many roads to one modification. Curr. Opin. Genet. Dev. *15*, 191–199.

Gao, F., Niu, Y., Sun, Y.E., Lu, H., Chen, Y., Li, S., Kang, Y., Luo, Y., Si, C., Yu, J., et al. (2017). De novo DNA methylation during monkey pre-implantation embryogenesis. Cell Res. *27*, 526–539.

Heinz, S., Benner, C., Spann, N., Bertolino, E., Lin, Y.C., Laslo, P., Cheng, J.X., Murre, C., Singh, H., and Glass, C.K. (2010). Simple combinations of lineage-determining transcription factors prime cis-regulatory elements required for macrophage and B cell identities. Mol. Cell *38*, 576–589.

Hörmanseder, E., Simeone, A., Allen, G.E., Bradshaw, C.R., Figlmüller, M., Gurdon, J., and Jullien, J. (2017). H3K4 methylation-dependent memory of somatic cell identity inhibits reprogramming and development of nuclear transfer embryos. Cell Stem Cell *21*, 135–143.e6.

Huang, W., Sherman, B.T., and Lempicki, R.A. (2009). Systematic and integrative analysis of large gene lists using DAVID bioinformatics resources. Nat. Protoc. *4*, 44–57.

Inoue, K., Kohda, T., Sugimoto, M., Sado, T., Ogonuki, N., Matoba, S., Shiura, H., Ikeda, R., Mochida, K., Fujii, T., et al. (2010). Impeding Xist expression from the active X chromosome improves mouse somatic cell nuclear transfer. Science *330*, 496–499.

Kishigami, S., Mizutani, E., Ohta, H., Hikichi, T., Thuan, N.V., Wakayama, S., Bui, H.T., and Wakayama, T. (2006a). Significant improvement of mouse cloning technique by treatment with trichostatin A after somatic nuclear transfer. Biochem. Biophys. Res. Commun. *340*, 183–189.

Kishigami, S., Van Thuan, N., Hikichi, T., Ohta, H., Wakayama, S., Mizutani, E., and Wakayama, T. (2006b). Epigenetic abnormalities of the mouse paternal zygotic genome associated with microinsemination of round spermatids. Dev. Biol. *289*, 195–205.

Langfelder, P., and Horvath, S. (2008). WGCNA: an R package for weighted correlation network analysis. BMC Bioinformatics *9*, 559.

Liu, W., Liu, X., Wang, C., Gao, Y., Gao, R., Kou, X., Zhao, Y., Li, J., Wu, Y., Xiu, W., et al. (2016). Identification of key factors conquering developmental arrest of somatic cell cloned embryos by combining embryo biopsy and single-cell sequencing. Cell Discov. *2*, 16010.

Liu, Z., Cai, Y., Wang, Y., Nie, Y., Zhang, C., Xu, Y., Zhang, X., Lu, Y., Wang, Z., Poo, M., and Sun, Q. (2018). Cloning of macaque monkeys by somatic cell nuclear transfer. Cell *172*, 881–887.e7.

Macfarlan, T.S., Gifford, W.D., Driscoll, S., Lettieri, K., Rowe, H.M., Bonanomi, D., Firth, A., Singer, O., Trono, D., and Pfaff, S.L. (2012). Embryonic stem cell potency fluctuates with endogenous retrovirus activity. Nature *487*, 57–63.

Matoba, S., and Zhang, Y. (2018). Somatic cell nuclear transfer reprogramming: mechanisms and applications. Cell Stem Cell *23*, S1934-5909(18)30300-X.

Matoba, S., Inoue, K., Kohda, T., Sugimoto, M., Mizutani, E., Ogonuki, N., Nakamura, T., Abe, K., Nakano, T., Ishino, F., and Ogura, A. (2011). RNAi-mediated knockdown of Xist can rescue the impaired postimplantation development of cloned mouse embryos. Proc. Natl. Acad. Sci. USA *108*, 20621–20626.

Matoba, S., Liu, Y., Lu, F., Iwabuchi, K.A., Shen, L., Inoue, A., and Zhang, Y. (2014). Embryonic development following somatic cell nuclear transfer impeded by persisting histone methylation. Cell *159*, 884–895.

Matoba, S., Wang, H., Jiang, L., Lu, F., Iwabuchi, K.A., Wu, X., Inoue, K., Yang, L., Press, W., Lee, J.T., et al. (2018). Loss of H3K27me3 Imprinting in Somatic Cell Nuclear Transfer Embryos Disrupts Post-Implantation Development. Cell Stem Cell *23*. Published online July 19, 2018. https://doi.org/10.1016/j.stem.2018.06.008.

Peaston, A.E., Evsikov, A.V., Graber, J.H., de Vries, W.N., Holbrook, A.E., Solter, D., and Knowles, B.B. (2004). Retrotransposons regulate host genes in mouse oocytes and preimplantation embryos. Dev. Cell *7*, 597–606.

Peat, J.R., and Reik, W. (2012). Incomplete methylation reprogramming in SCNT embryos. Nat. Genet. *44*, 965–966.

Sun, D., Xi, Y., Rodriguez, B., Park, H.J., Tong, P., Meong, M., Goodell, M.A., and Li, W. (2014). MOABS: model based analysis of bisulfite sequencing data. Genome Biol. *15*, R38.

Tachibana, M., Amato, P., Sparman, M., Gutierrez, N.M., Tippner-Hedges, R., Ma, H., Kang, E., Fulati, A., Lee, H.S., Sritanaudomchai, H., et al. (2013). Human embryonic stem cells derived by somatic cell nuclear transfer. Cell *153*, 1228–1238.

Tang, F., Barbacioru, C., Nordman, E., Li, B., Xu, N., Bashkirov, V.I., Lao, K., and Surani, M.A. (2010). RNA-seq analysis to capture the transcriptome landscape of a single cell. Nat. Protoc. *5*, 516–535.

Teperek, M., and Miyamoto, K. (2013). Nuclear reprogramming of sperm and somatic nuclei in eggs and oocytes. Reprod. Med. Biol. *12*, 133–149.

Trapnell, C., Pachter, L., and Salzberg, S.L. (2009). TopHat: discovering splice junctions with RNA-seq. Bioinformatics *25*, 1105–1111.

Trapnell, C., Williams, B.A., Pertea, G., Mortazavi, A., Kwan, G., van Baren, M.J., Salzberg, S.L., Wold, B.J., and Pachter, L. (2010). Transcript assembly and quantification by RNA-seq reveals unannotated transcripts and isoform switching during cell differentiation. Nat. Biotechnol. *28*, 511–515.

Van Thuan, N., Bui, H.T., Kim, J.H., Hikichi, T., Wakayama, S., Kishigami, S., Mizutani, E., and Wakayama, T. (2009). The histone deacetylase inhibitor scriptaid enhances nascent mRNA production and rescues full-term development in cloned inbred mice. Reproduction *138*, 309–317.

Velasco, G., Hubé, F., Rollin, J., Neuillet, D., Philippe, C., Bouzinba-Segard, H., Galvani, A., Viegas-Péquignot, E., and Francastel, C. (2010). Dnmt3b recruitment through E2F6 transcriptional repressor mediates germ-line gene silencing in murine somatic tissues. Proc. Natl. Acad. Sci. USA *107*, 9281–9286.

Wakayama, T., Perry, A.C.F., Zuccotti, M., Johnson, K.R., and Yanagimachi, R. (1998). Full-term development of mice from enucleated oocytes injected with cumulus cell nuclei. Nature *394*, 369–374.

Wang, H., and Dey, S.K. (2006). Roadmap to embryo implantation: clues from mouse models. Nat. Rev. Genet. *7*, 185–199.

Wang, F., Kou, Z., Zhang, Y., and Gao, S. (2007). Dynamic reprogramming of histone acetylation and methylation in the first cell cycle of cloned mouse embryos. Biol. Reprod. *77*, 1007–1016.

Wang, L., Zhang, J., Duan, J., Gao, X., Zhu, W., Lu, X., Yang, L., Zhang, J., Li, G., Ci, W., et al. (2014). Programming and inheritance of parental DNA methylomes in mammals. Cell *157*, 979–991.

Wang, C., Liu, X., Gao, Y., Yang, L., Li, C., Liu, W., Chen, C., Kou, X., Zhao, Y., Chen, J., et al. (2018). Reprogramming of H3K9me3-dependent heterochromatin during mammalian embryo development. Nat. Cell Biol. *20*, 620–631.

Wei, Y., Huan, Y., Shi, Y., Liu, Z., Bou, G., Luo, Y., Zhang, L., Yang, C., Kong, Q., Tian, J., et al. (2011). Unfaithful maintenance of methylation imprints due to loss of maternal nuclear Dnmt1 during somatic cell nuclear transfer. PLoS ONE *6*, e20154.

Wilmut, I., Schnieke, A.E., McWhir, J., Kind, A.J., and Campbell, K.H.S. (1997). Viable offspring derived from fetal and adult mammalian cells. Nature *385*, 810–813.

Xi, Y., and Li, W. (2009). BSMAP: whole genome bisulfite sequence MAPping program. BMC Bioinformatics *10*, 232.

Xue, Z., Huang, K., Cai, C., Cai, L., Jiang, C.Y., Feng, Y., Liu, Z., Zeng, Q., Cheng, L., Sun, Y.E., et al. (2013). Genetic programs in human and mouse early embryos revealed by single-cell RNA sequencing. Nature *500*, 593–597.

Yang, X., Smith, S.L., Tian, X.C., Lewin, H.A., Renard, J.P., and Wakayama, T. (2007). Nuclear reprogramming of cloned embryos and its implications for therapeutic cloning. Nat. Genet. *39*, 295–302.

Zhu, P., Guo, H., Ren, Y., Hou, Y., Dong, J., Li, R., Lian, Y., Fan, X., Hu, B., Gao, Y., et al. (2018). Single-cell DNA methylome sequencing of human preimplantation embryos. Nat. Genet. *50*, 12–19.

STAR★METHODS

KEY RESOURCES TABLE

REAGENT or RESOURCE	SOURCE	IDENTIFIER
Chemicals, Peptides, and Recombinant Proteins		
Pregnant mare serum gonadotropin	San-Sheng pharmaceutical Co. Ltd	S160106
Human chorionic gonadotropin	San-Sheng pharmaceutical Co. Ltd	B151104
Bovine testicular hyaluronidase	Sigma	H4272
M2 medium	Sigma	M7167
Cytochalasin B	Sigma	C6762
G1 medium	Vitrolife	10128
Pronase E	Sigma	P8811
Albumin, Acetylated from bovine serum	Sgima	B8894
Dulbecco's Phosphate-Buffered Saline (DPBS)	ThermoFisher	14249-95
SuperScript III reverse transcriptase	ThermoFisher	18080-044
RNase Inhibitor	Ambion	AM2682
Terminal deoxynucleotidyl transferase (TdT)	ThermoFisher	10533-073
Unmethylated Lambda DNA	ThermoFisher	SD0021
Agencourt AMPure XP beads	Beckman Coulter	A63880
Critical Commercial Assays		
Pico Methyl-Seq Library Prep Kit	Zymo Research	D5456
KAPA Hyper Prep Kit	KAPA	KK8504
mMESSAGE mMACHINE T7 Ultra Kit	Life Technologies	AM1345
RNeasy Mini Kit	QIAGEN	74104
Deposited Data		
Raw and analyzed WGBS and RNA-seq data	This paper	GEO: GSE108711
Experimental Models: Organisms/Strains		
Mature DBA2 male mice	Charles River	N/A
Mature C57BL/6 female mice	Charles River	N/A
Mature C57BL/6 male mice	Charles River	N/A
Mature ICR female mice	Charles River	N/A
Oligonucleotides		
RT-qPCR primers (Table S2)	This paper	N/A
siRNA Targeting Sequences (Table S2)	This paper	N/A
Recombinant DNA		
pMD18+Kdm4b	This paper	accession number NM_001357909.1
pMD18+Kdm5b	This paper	accession number NM_152895.2
Software and Algorithms		
Tophat v1.3.3	(Trapnell et al., 2009)	https://ccb.jhu.edu/software/tophat/index.shtml
Cufflinks v1.2.0	(Trapnell et al., 2010)	http://cole-trapnell-lab.github.io/cufflinks/
bsmap v2.89	(Xi and Li, 2009)	http://dldcc-web.brc.bcm.edu/lilab/yxi/bsmap/bsmap-2.89.tgz
moabs v1.3.0	(Sun et al., 2014)	http://dldcc-web.brc.bcm.edu/lilab/deqiangs/moabs/moabs.html
STAR v2.5.2b	(Dobin et al., 2013)	https://github.com/alexdobin/STAR
HOMER v4.8.3	(Heinz et al., 2010)	http://homer.ucsd.edu/homer/
R v3.2.4	https://www.R-project.org/	https://www.R-project.org/
WGCNA package v 1.13	(Langfelder and Horvath, 2008)	https://labs.genetics.ucla.edu/horvath/htdocs/CoexpressionNetwork/Rpackages/WGCNA/

CONTACT FOR REAGENT AND RESOURCE SHARING

Further information and requests for resources and reagents should be directed to and will be fulfilled by the Lead Contact, Shaorong Gao (gaoshaorong@tongji.edu.cn).

EXPERIMENTAL MODEL AND SUBJECT DETAILS

Mice

B6D2F1 (C57BL/6 female x DBA2 male) female mice at 8-10 week-old were used as oocyte recipients. Cumulus cells (female) and sertoli cells (male) were collected from B6D2F1 background mice. Mouse embryonic fibroblast (MEF) cells were established from C57BL/6 background mouse embryos at 13.5 dpc. 9-15 week-old females from the ICR strain were used as recipients for embryo transplantation. All animal maintenance and experimental procedures were performed according to Tongji University Guide for the use of laboratory animals. Mouse were housed under a 12-h light/dark cycle under pathogen-free conditions at 22 ± 2°C and fed with free access to standard mouse chow and tap water.

Donor cell preparation

Both cumulus cells and oocytes were prepared by super-ovulating 8-10 week-old B6D2F1 female mice. Super-ovulation was induced by the sequential injection with 5 IU each of pregnant mare serum gonadotropin (PMSG) and human chorionic gonadotropin (hCG) at intervals of 48 hours. Cumulus-oocyte complexes (COCs) were collected from oviducts 14 hours after hCG injection and treated with bovine testicular hyaluronidase to obtain dissociated cumulus cells and oocytes, respectively.

Sertoli cells were collected from testes of 3- to 5- day-old B6D2F1 male mice. Testicular masses were incubated in PBS containing 1mg/ml collagenase at 37°C for 10 minutes to obtain the dissociated sertoli cells.

Mouse embryonic fibroblasts were established from C57BL/6 background mouse embryos at 13.5 dpc. After removal of head and all organs, minced tissue from remaining corpus was dissociated in Trypsin-EDTA and then diluted with equal amount of DMEM containing 10% FBS to terminate digestion. The cell suspension was cultured to harvest for the primary MEF cells. MEF cells were used for experiments after one passage.

METHOD DETAILS

Somatic cell nuclear transfer and embryo culture

MII oocytes were collected from super-ovulated adult BDF1 females. The oocytes were enucleated in M2 medium containing 5 μg/mL cytochalasin B (CB) by Piezo-driven pipette (PrimeT 130 ech) of an Olympus inverted microscope. The nuclei of donor cumulus cells were transferred into enucleated oocytes by direct injection, and activated in Ca^{2+}-free CZB containing 1mM $SrCl_2$ and 5 μg/mL CB for 5 hours. Reconstructed embryos were thoroughly washed and cultured in G1 medium with amino acids at 37°C in humidified atmosphere of 5% CO_2. SCNT experiment was performed at least twice for each treatment condition.

In vitro transcription of mRNA and direct injection

Mouse *Kdm4b* and *Kdm5b* mRNA were cloned into T7-driven vectors, and mRNAs were synthetized *in vitro* using mMESSAGE mMACHINE T7 Ultra Kit following the manufacturer's instructions. The final concentration of mRNA was diluted to 100 ng/μL before injection. Enucleated oocytes were injected with ~10pL of mRNA using a Piezo-driven micromanipulator. Primers were shown in Table S2.

Knockdown of Dnmt3a/3b in cloned embryo

siRNAs against *Dnmt3a* and *Dnmt3b* were diluted in nuclease free water at a final concentration of 10 μM stock solutions. Primers were shown in Table S2. Enucleated oocytes were injected with ~10pL of 10 μM siRNAs for *Dnmt3a* or *Dnmt3b* using a Piezo-driven micromanipulator. After incubating for 30 minutes in G1 medium, the nuclei of donor cells were transferred into the pre-treated enucleated oocytes by direct injection.

Reverse transcription and quantitative RT-PCR analysis

To analyze knockdown efficiency of siRNA, total RNA of 20 embryos at 4-cell stage were purified using RNeasy mini kit according to manufacturer's instruction. The cDNA was synthesized using 5X All-in-One RT MasterMix (abm). Quantitative RT-PCR was performed using a SYBR Premix Ex Taq (Takara) and signals were detected with ABI7500 Real-Time PCR System (Applied BioSystems). *Gapdh* was used as endogenous control. Primers were shown in Table S2.

Embryo transfer

The mRNA/siRNA-injected and control SCNT embryos at 2-cell stage were transferred into the oviduct of pseudo-pregnant female mice, respectively. Caesarean section was carried out at day 19.5 and the surviving pups were fostered by lactating ICR females.

Biopsy culture system

This section was adapted from (Liu et al., 2016). In brief, the zona pellucida of injected and control SCNT embryos was removed with 0.5% pronase E. After incubating 2- or 4-cell stage embryos in Ca^{2+}-free CZB medium, one blastomere was removed by gently pipetting using a fire-polished glass needle with an inner diameter of 120 μm. The single separated blastomere was harvested and frozen, and the rest were still cultured at 37°C in humidified atmosphere of 5% CO2 until the blastocyst stage. We then pooled at least 30-50 separated blastomeres together at each individual cleaved stage (including either arrest or to blast samples) for the following library construction. The tight junctions of TE cells and ICM cells were separated by gently pipetting in a pipette with a diameter of 40-60 μm. All samples were washed several times in 0.5% BSA-PBS solution before they were prepared for library generation.

WGBS library preparation

For WGBS, 30-50 cells were used per reaction. All isolated cells were washed three times in 0.5% BSA-PBS solution to avoid possible contamination. The sequencing libraries were generated using the Pico Methyl-Seq Library Prep Kit following the manufacturer's instructions. Paired-end 150-bp sequencing was performed on a NovaSeq (Illumina) at Berry Genomics Corporation.

Generation of RNA-Seq library

The RNA-seq method followed previously published studies (Tang et al., 2010). Briefly, reverse transcription was performed directly on the cytoplasmic lysate of indicated samples. Terminal deoxynucleotidyl transferase (TdT) was then used to add a poly(A) tail to the 3′ end of the first-strand cDNAs. The total cDNA library was then amplified by 18- 20 cycles for the library construction. The amplified cDNA was fragmented, and then KAPA Hyper Prep Kit was used to generate sequence libraries. Paired-end 125-bp or 150-bp sequencing was further performed on a HiSeq 2500 or NovaSeq (Illumina) at Berry Genomics Corporation. 2 or 3 biological replicates were analyzed for each treatment condition.

QUANTIFICATION AND STATISTICAL ANALYSIS

Biological replicates

A single pooled sample (30-50 embryos) was used for WGBS analysis in each treatment condition due to the technical difficulty in preparing enough number of SCNT embryos. 2 or 3 biological replicates (10 embryos pooled together per sample) were analyzed for RNA-seq in each treatment condition.

To analyze the developmental outcome, 2-4 independent experiments were performed. 30 to 187 2-cell embryos were analyzed for pre-implantation development of SCNT embryos. 25 to 95 2-cell embryos were transferred to pseudopregnant female mice to examine post-implantation development. 2 to 12 placentae were examined for their weight and histology. See also Tables S3 and S4.

Statistical analysis

The developmental data are represented as the mean with the SEM (standard error of the mean). Statistical significance was calculated using Student's t test.

Mapping and quantification of RNA-seq and WGBS data

Sequencing reads from the low input RNA-seq samples were mapped to the mm9 reference genome using Tophat (v1.3.3) (Trapnell et al., 2009). Expression levels for all RefSeq transcripts were quantified to FPKM using Cufflinks (v1.2.0) (Trapnell et al., 2010), and FPKM values of replicates were averaged for downstream analysis. All the low input BS-seq reads were first processed using TrimGalore (v0.3.3) to remove adaptor and low-quality reads. Then mapped to a combined genome with mm9 and 48052 lambda sequence using bsmap (v2.89) (Xi and Li, 2009). Methylation level of each CpG sites was estimated using mcall (Sun et al., 2014). As biological replicates of the same treatment and developmental stage were highly correlated based on methylation level, we combined them for the downstream analysis. The methylation level of same CpG site from multiple replicates was determined using total methylated reads count across replicates versus total reads count across replicates, and CpG sites with less than 3 reads were discarded.

Expression and methylation level quantification of repeats elements

To assess the expression level of repeats elements, all the RNA-seq files were re-mapped to the mm9 genome using the STAR aligner software allowing up to 3 mismatches and filtering out reads mapping to more than 500 positions in the genome (Dobin et al., 2013). Mapped files were then processed using the makeTagDirectory script of HOMER with -keepOne option (Heinz et al., 2010). The tag directories of the mapped files were analyzed using the analyzeRepeats.pl script of HOMER with the option 'repeat' and -noadj. This script adds the reads that map to multiple loci to the expression of the repeat class they represent, which were summarized to 1221 repeat types. Total reads count of each sample was normalized to 1 million and replicate were averaged for comparison. To analyze the methylation level of repeat elements, we downloaded the repeat annotations from the UCSC table browser. DNA methylation level was calculated for each repeat annotation and values of the same repeat types were averaged.

DMR calling and classification

We used mcomp function in the moabs software (v1.3.0) to generate the differential methylated regions(DMRs) between different conditions (Sun et al., 2014). The DMRs were generated using M2 method, which based on the credible methylation difference metric. The DMC is defined as cMethDif > 0.2, and DMR is defined as minC > = 3, maxDist 300 and cMethDif > 0.2. As the DMRs generated by mcomp are in different length, for fair comparison of the DMR number and clustering analysis, we divided the DMRs into 300bp bins and performed the downstream analysis, regions less than 300bp are regarded as 300bp.

To define the de-methylated (dDMR), re-methylated (rDMR) and persisted (pDMR) DMRs in NT 2-cell arrest samples. We first performed DMR analysis between NT 2-cell arrest samples and fertilized 2-cell samples. For each hyper-methylated DMR in this comparison (NT 2-cell arrest > fertilized 2-cell), we calculated the averaged DNA methylation level of NT 1-cell, NT 2-cell arrest, NT 2-cell to blastocyst and fertilized 2-cell on this DMR, and defined the rescue score(RS) using the formation below.

$$RS = abs(Methyl_{NT\ Sample} - Methyl_{Fertilized\ Sample}) - \lambda * abs(Methyl_{NT\ 2-cell\ arrest} - Methyl_{Fertilized\ Sample}).$$

For 2-cell and 4-cell stage, λ was set to 0.5, for blastocyst stage, λ was set to 1. If RS $\leq$ 0, this DMR was regarded as rescued in this sample type, and if RS > 0, this DMR was regarded as unchanged in this sample type, thus we can define the three types of DMRs as follows,

dDMR: rescued in NT 2-cell to blastocyst samples;
rDMR: rescued in NT 1-cell samples, but unchanged in NT 2-cell to blastocyst samples;
pDMR: unchanged in both NT 1-cell samples and NT 2-cell to blastocyst samples.

Heatmaps were generated using pheatmap function in R. The row of the heatmaps were clustered based on the RS score using kmeans function in R. Similar calculations were made to define the three types of DMRs in NT 4-cell arrest samples, NT ICM and TE samples.

To link the de-methylation, re-methylation and persist-methylation to genes and repeats, we calculated the averaged DNA methylation level of promoter regions (defined as ± around TSS) and repeats types. Similar RS score can be calculated based on the promoter and repeats methylation level. For 2-cell and 4-cell stage, λ was set to 0.5, for blastocyst stage, λ was set to 1. And the de-methylated, re-methylated and persisted methylated genes and repeats were defined similar to DMRs.

Donor-specific DMR definition

To generate donor-specific DMRs, we first called hyper DMRs between SCNT embryo from different donors and fertilized embryos by mcomp, the DMRs were divided into 300bp regions for downstream comparison. We classified DMRs at 2-cell and 4-cell stage into rDMRs and pDMRs by RS score, and MEF specific rDMRs/pDMRs were rDMRs/pDMRs that only present in MEF hyper DMRs, similar definitions were used for sertoli (SC) and cumulus cell (CC) specific rDMRs/pDMRs. The donor-shared rDMRs/pDMRs were the rDMRs/pDMRs that presented in both donor cell type hyper DMRs. Heatmaps were generated using pheatmap function in R. The row of the heatmaps was clustered based on the donor cell type specificity.

Genomic annotations and enrichment calculation

We downloaded the RefSeq transcript annotation and repeats annotation from the USCS table browser (http://genome.ucsc.edu/cgi-bin/hgTables). The enrichment of DMRs in different genome context were calculated using observed ratio versus expected ratio, where the observed ratio is the number of bps of certain class of DMRs overlapped with a specific genome context versus total length of certain class of DMRs; and the expected ratio if the number of bps of a specific genome context versus the genome length.

WGCNA analysis

The Weighted gene co-expression network analysis were performed using WGCNA package in R (Langfelder and Horvath, 2008). We choose five time points, the oocyte, 2-cell, 4-cell, ICM and TE to perform the analysis. Both the fertilized and SCNT datasets were independently constructed using a previously published procedure (Xue et al., 2013), setting the power beta = 10. We use the Dynamic Hybrid Tree Cut algorithm to cut the hierarchal clustering tree and defined modules as branches from the tree cutting. The modules with highly correlated eigengenes (correlation above 0.7) were merged. After constructing the modules for fertilized and SCNT datasets, we performed hub gene overlap analysis between the fertilized and SCNT modules. Overlap between modules was evaluated using hypergeometric test, number of overlapped genes and p values are labeled on heatmaps, and names of each module were determined based on their expression pattern across the developmental stage.

Consistency analysis between DNA methylation and gene expression

We performed consistency analysis on genes and repeats to determine the DNA methylation affected gene and repeat sets. The DNA methylation level on gene were calculated on promoter regions (defined as ± around TSS), and the DNA methylation level on repeats were calculated on each repeat annotation and averaged for the same type of repeats (MERVL-int etc). For each developmental stage, we compared the difference of DNA methylation level and expression level between SCNT and fertilized embryo samples, genes or repeats with concordant change of DNA methylation level and gene expression level are defined as DNA methylation affected gene or repeat sets for each stage. For 2-cell and 4-cell stage, we defined the concordant change threshold as DNA

methylation level increase 0.2, expression level decrease 1 or DNA methylation level decrease 0.2, expression level increase 1. For ICM and TE stage, we defined the concordant change threshold as DNA methylation level increase 0.1, expression level decrease 1 or DNA methylation level decrease 0.1, expression level increase 1. For repeats, the expression level threshold was defined as 0.2, and the methylation level threshold was the same with genes.

Gene ontology analysis

Functional annotation was performed using the Database for Annotation, Visualization and Integrated Discovery(DAVID) Bioinformatics Resource (Huang et al., 2009). We used the R package GO.db, KEGG.db, GOstats and org.Mm.eg.db to perform the GO enrichment analysis. Gene ontology terms for each function cluster were summaries to a representative term and P values were plotted to show the significance.

DATA AND SOFTWARE AVAILABILITY

The accession number for the RNA-seq and WGBS data reported in this paper is GEO: GSE108711. The accession numbers for the public SCNT RNA-seq and fertilized WGBS data reported in this paper are GEO: GSE56697, GEO: GSE70605, and GEO: GSE97778 (Liu et al., 2016; Wang et al., 2018; Wang et al., 2014).